

# **FATIGUE BEHAVIOR OF CFRP-STRENGTHENED REINFORCED CONCRETE BRIDGE GIRDERS**

John Aidoo, University of South Carolina, Columbia, SC  
Dr. Kent A. Harries, University of South Carolina, Columbia, SC  
Dr. Michael F. Petrou, University of South Carolina, Columbia, SC

## **Abstract**

Although many tests have been conducted investigating strengthening reinforced concrete members with FRP materials, there are still many aspects of their use that remain to be investigated. The fatigue behavior of reinforced concrete beams strengthened with FRP composite sheets and strips, for instance, which is described in this paper, provides valuable information regarding the expected long-term performance of the FRP strengthening systems.

The present study examines the effects of one-dimensional FRP composite rehabilitation systems on the flexural fatigue performance of reinforced concrete bridge girders. Experiments are being conducted on reinforced concrete tee-beams with and without bonded FRP reinforcement on their tensile surfaces. The objective of this investigation is to determine whether such external FRP repair methods are able to resist fatigue loads and to establish the effect that these repair systems have on the fatigue behavior and remaining life of the girders.

Eight 508 mm deep reinforced concrete tee-beams having 5.6 m clear spans were tested with a concentrated load at midspan under constant amplitude cyclic loading. The details of these beams represent a 62% scaling of full-scale beams, removed from a 1961 Interstate, to be tested in 2002. Two commercially available CFRP repair systems were used to retrofit the stem soffits of the girders. The two retrofit systems were designed such that their stiffness was approximately equivalent.

Results from the fatigue tests are presented with particular attention paid to the FRP-concrete interface and its significant degradation and eventual failure under fatigue loading conditions.

## **Introduction**

Although many tests have been conducted investigating strengthening reinforced concrete members with FRP materials, there are still many aspects of their use that remain to be investigated. Little is known of the fatigue performance of such materials, and considerable investigation of their long-term performance is necessary before FRP materials gain full acceptance as civil infrastructure materials.

There is a considerable body of work investigating the fatigue behavior of steel-reinforced concrete (Mallet, 1991). In general, it is concluded that the fatigue behavior of reinforced concrete is controlled by the fatigue behavior of the reinforcing steel. Furthermore, the nature of reinforced concrete design for fatigue generally maintains the transitive stresses in the longitudinal steel at a level well below the fatigue limit.

Helgason and Hanson (1974) present a well-accepted model of the fatigue behavior of reinforcing steel in tension tested in air. Moss (1982) provides a model of the fatigue behavior of reinforcing steel in concrete beams subject to flexure.

There has been very little investigation of the fatigue behavior of reinforced concrete beams having FRP retrofits. Meier (1992), Barnes and Mays (1999), Shahawy and Beitleman (1999) and Papakonstantinou et al. (2000) all report tests of reinforced concrete beams, retrofit with FRP subject to

fatigue loads. In all cases, the eventual fatigue failure has been similar to that of unretrofit beams, that is; controlled by fatigue of the longitudinal steel reinforcement. The observed increases in fatigue life are all attributed to the applied FRP relieving the stress demand on the existing steel. Papakonstantinou et al. demonstrated this clearly with tests designed to ensure that the internal steel reinforcement was subject to the same stresses for both retrofit and unretrofit specimens. In this case, no discernable difference between specimens having the same stress levels was observed.

## Objective

The objective of the present study is to investigate the fatigue behavior of large-scale reinforced concrete bridge girders retrofit with carbon fiber reinforced polymer (CFRP) composite materials. Particular attention is paid to the bond between the CFRP and concrete substrate. In this study, the influence of the retrofit on the fatigue life of the member is investigated, thus applied loads, rather than internal stresses, are maintained constant.

## Experimental Investigation

Eight 6100 mm long reinforced concrete tee beams were prepared for this investigation. The beams, whose details are shown in Figure 1, were 508 mm deep having a 102 mm thick by 559 mm wide flange and a 209 mm wide stem. The details of these beams represent a 62% scaling of full-scale beams, removed from a 1961 Interstate bridge, to be tested, beginning in 2002.

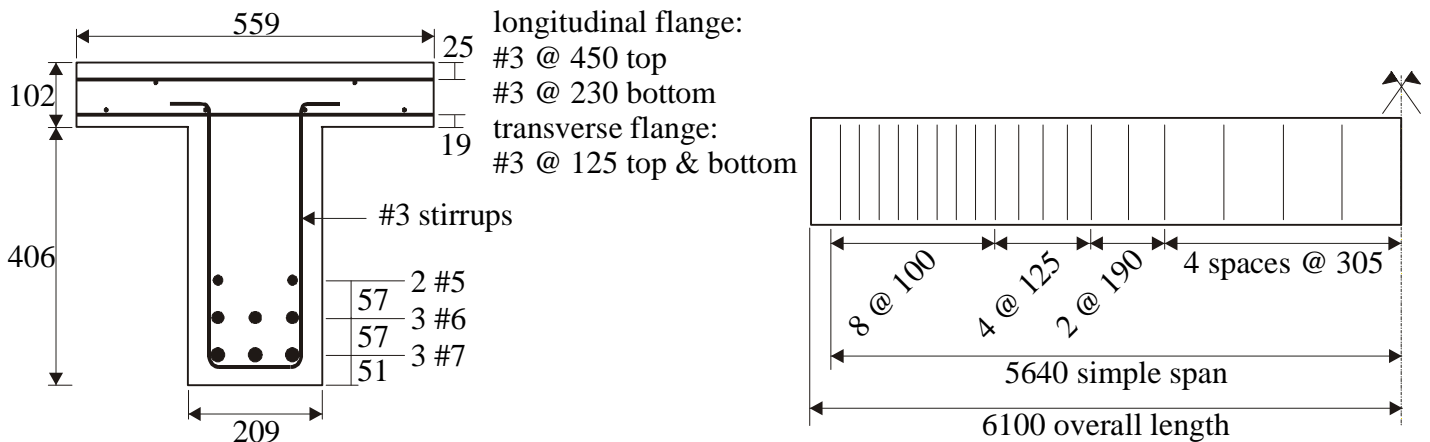


**Figure 1.** Test specimen details

A Type I concrete mix having a specified 28-day strength of 24 MPa was used for all beams. The beams were cast in pairs and the actual 28-day concrete strengths obtained are given in Table 1. All steel was Grade 60 deformed reinforcing bars. The yield and tensile strengths of the #7 bars comprising the lowest layer of longitudinal reinforcement are 439 MPa and 740 MPa, respectively.

Four beams were retrofit with CFRP materials on the soffit of the tee beam stem. The retrofit extended the length of the beam but did not extend under the supports. No additional anchorage, apart from the adhesive system was used. Two different CFRP systems were used. The remaining beams were left unretrofit and used as control specimens. Specimens were designated U1 through U4 for the unretrofit beams and RS1 and RS2 for those retrofit with the “strip” retrofit system and RF1 and RF2 for those with the “fabric” system (see below). Specimen U1 was a control specimen, tested in monotonic

midpoint flexure to failure in order to establish a backbone response. The remaining specimens were all tested under fatigue conditions.

**Retrofit Materials**

Two commercially available retrofit systems were used as indicated in Table 1. The “strip” system is a 102 mm wide preformed CFRP plate applied to the beam using an epoxy-based adhesive. Each strip has a tensile capacity of 540 kN and a tensile stiffness (EA) of 30000 kN. A single 102 mm wide strip was applied to the stem soffit of each RS beam.

The “fabric” system used is a hand-layed up unidirectional CFRP fabric applied using typical hand lay-up procedures. In order to compare the “strip” and “fabric” systems, a comparable “fabric” retrofit was designed based on the modular ratio of the materials. Two 203 mm wide layers of “fabric” were applied to the stem soffit of the RF beams. As shown in Table 1, the stiffness of the resulting retrofit was almost the same as that using the “strip” system. All Retrofit materials were applied following the manufacturer’s recommended procedure and directed by a technician provided by the manufacturer.

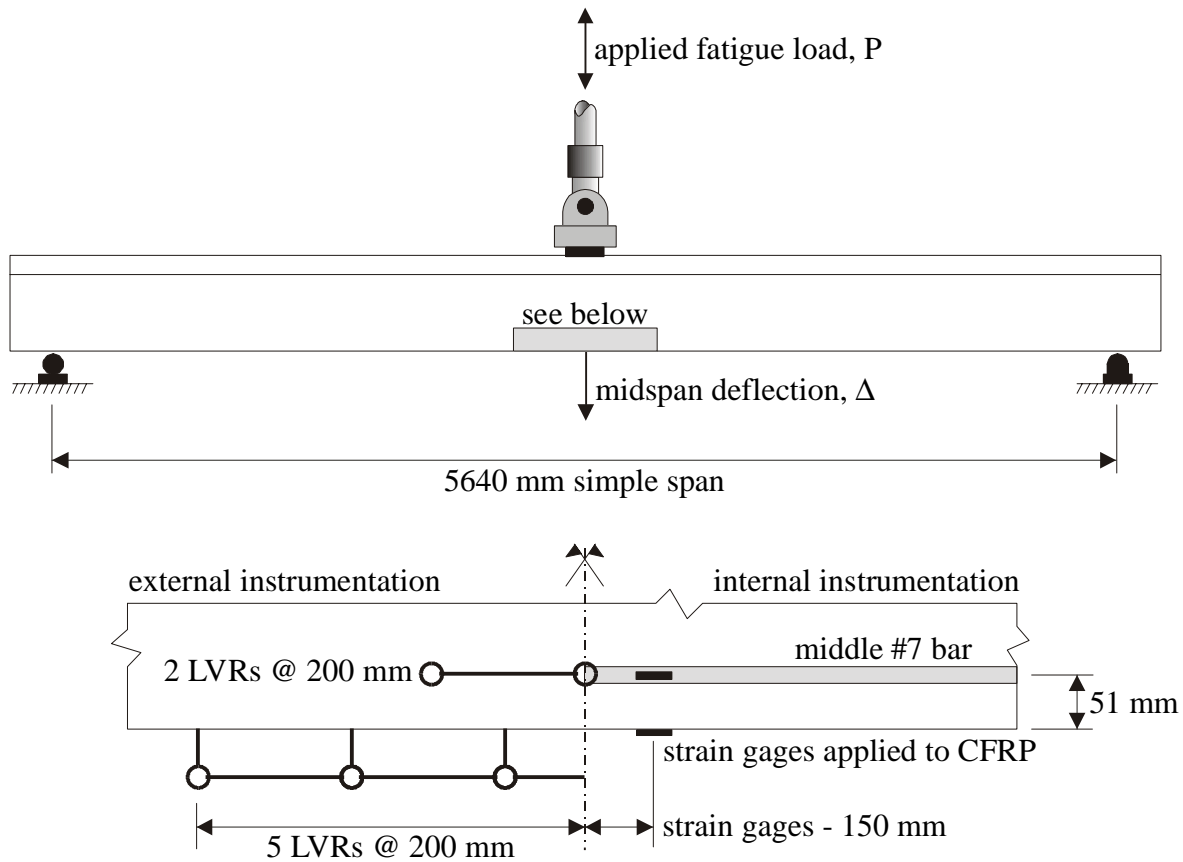


**Figure 2.** Test set-up and instrumentation

**Test Set-up and Instrumentation**

All beams were tested under midpoint flexure over a span of 5640 mm as shown in Figure 2. Fatigue tests were carried out in load control with sinusoidal applied loads being cycled at 1 Hz from a nominal value to a maximum value as indicated in “test control parameters” in Table 1.

A monotonic cycle was conducted prior to fatigue cycling (N = 1) to establish the initial behavior of each specimen. Monotonic cycles, with full instrumentation, were conducted periodically throughout

the fatigue life. These tests were conducted, initially at short intervals (a few hundred to a few thousand cycles) and then at intervals of approximately 80000 cycles.

Each specimen was instrumented with internal strain gages on the #7 reinforcing steel. These gages were operational during the first few cycles and were used to determine reinforcing steel stresses at  $N = 1$ . External linear variable resistor (LVR) instruments were used to capture beam curvature and strains at both the stem soffit and at the level of the #7 reinforcing steel. A precision linear variable displacement transducer was used to measure midspan deflection and a load cell, integrated into the actuator system, was used to record loads and control the test. A schematic of the instrumentation provided is shown in Figure 2.

### ***Predicted Fatigue Behavior***

As stated previously, the objective of this study is to investigate the fatigue behavior of CFRP retrofit beams. In order to develop a test program, reasonable predictions of the beam response and fatigue life are necessary. These are presented in Table 1. The goal of the experimental program was to retrofit reinforced concrete beams under a “high stress range”, whose fatigue life may be less than  $10^5$  cycles. The “low stress range” was selected to result in an unretrofit fatigue life of approximately  $10^6$  cycles.

Predicted beam behavior and reinforcing steel stresses were determined using the plane sections analysis program RESPONSE 2000 (Bentz, 2000). The FRP material properties were modeled directly in this program, however it is noted that the predicted behavior assumes perfect bond between the FRP and concrete substrate. This assumption is valid for low values of  $N$ .

The predicted number of cycles to failure,  $N_1$  (failure is defined as the first rupture of a reinforcing bar) was determined using the following equation proposed by Helgason and Hanson (1974).

$$\log(N_1) = 6.969 - 0.00555S \quad (\text{EQ 1})$$

Where  $S$  = stress range in reinforcing steel in MPa. Because Equation 1 is calibrated based on the tensile fatigue behavior of reinforcing steel in air, it was felt that the results would represent an extreme lower bound solution. Indeed, this is in fact what was found.

Based on the predictions made and the results of the control specimen, U1, the test control parameters shown in Table 1 were selected. Each specimen in a series was subject to these forces which were selected to develop the target stress range in the #7 reinforcing steel.

## **Experimental Results**

Experimentally observed strains and stresses in the #7 reinforcing steel, midspan deflections and fatigue life are shown in Table 1. Applied moment versus midspan deflection behavior for selected cycles are shown in Figure 3. In these data, failure is assumed to correspond to the number of cycles at which the first reinforcing bar ruptured ( $N_1$ ). Since the stresses are below yield in the other reinforcing bars, the specimens are still able to carry the applied loads. The values of  $N_2$ ,  $N_3$  and  $N_4$  correspond to the cycle at which the second, third and fourth bar ruptured, respectively. In all cases,  $N_1$  represents the rupture of one of the lower layer of #7 bars.

Figure 3(a) shows the monotonic response to failure of Specimen U1. This beam behaved as would be expected for an under reinforced concrete beam. The cracked stiffness of the beam is approximately constant through the initial yield of the extreme tension layer of reinforcing steel. As the curvature increases and more steel yields, the behavior exhibits a clear change on stiffness. This is noted as “general yield” and occurred at a midspan deflection of 26.9 mm. Considerable flexural ductility was exhibited until the compression concrete began crushing resulting in a rapid loss of load carrying

capacity. This occurred at a midspan deflection of 107 mm or a flexural displacement ductility of 4. No fracture of reinforcing steel was observed.

The responses of the fatigue-loaded specimens at various values of  $N$  are shown in Figures 3(b) through (f). In each case, the cycle at  $N = 1$  and at  $N = N_1$  are shown. Intervening cycles are shown to give an indication of damage accumulation. Values of  $N$  at reinforcing bar ruptures ( $N_n$ ) were determined exactly for the ultimate reported rupture when the reinforcing bar rupture resulted in sufficient loss of capacity or stiffness to trigger the loading actuator to stop. For initial reinforcing bar ruptures, where the loss of capacity or stiffness was insufficient to trigger the loading actuator to stop, the values of  $N$  were determined from recorded deflection and strain data. In these cases, the value of  $N$  is reported with a precision of approximately 10000 cycles.

### ***High Stress Series (Specimens U2, RS1 and RF1)***

Specimens U2, RF1 and RS1 were tested at a high stress level resulting in relatively short fatigue lives. Specimen U1 failed after  $1.9 \times 10^5$  cycles as did RF1. Specimen RF1 failed at just over  $3 \times 10^5$  cycles. These specimens were tested at an applied load of approximately 80% of the observed yield value of Specimen U1. At this load level, the extreme tension reinforcement (#7 bars) may be expected to be just approaching their yield value. Indeed strain gages on the #7 bars indicated a peak strain of 2280 microstrain during the cycle at  $N = 1$ , slightly higher than the yield strain of 2195 microstrain.

Tested at the same applied load level, the observed strains in the reinforcing steel were lower in the retrofit specimens, 1900 microstrain, indicating that during the initial cycle, bond between the CFRP and concrete substrate was sound. As cycling progressed, shear cracks widened. (It is noted that the shear capacity of the test specimens is barely adequate for the midspan loading case, the details were maintained, however, in order to match the Interstate bridge prototype to be tested later.) The relatively large shear deformations near the region of greatest moment (midspan) resulted in the initiation of delamination of the CFRP retrofit. This delamination initiated near the midspan and progressed toward the support on the same side of midspan. This delamination will be discussed at greater length below.

Initial failure of all the fatigue specimens was through rupture of a #7 bar at cycle  $N_1$ . Despite, the increasing permanent deflections evident in the beams (see Figure 3), failure occurred at a midspan deflection less than that corresponding to general yield of Specimen U1. If the beam was still able to carry the applied loads, the fatigue loading was continued through further bar ruptures until the beam could no longer support the applied load. A secondary failure, driven by the energy release of the bar rupture, typically involved the complete delamination, from midspan to one support, of the CFRP retrofit.

### ***Low Stress Series (Specimens U4, RS2 and RF2)***

Specimens U4, RF2 and RS2 were tested at a lower stress level resulting in longer fatigue lives. Specimen U4 failed after  $7.1 \times 10^5$  cycles. Specimens RS2 and RF2 each sustained over  $1 \times 10^6$  cycles. These specimens were tested at an applied load of approximately 63% of the observed yield value of Specimen U1. At this load level, the extreme tension reinforcement, also, only experienced approximately 60% of its yield stress.

Similar to the high stress range, initial bond between the CFRP and concrete was good although delaminations, driven by shear deformations, were observed. These delaminations progressed with cycling and the eventual failure of the specimens was similar to the high stress specimens. Midspan deflections at failure, were lower than those reported for the high stress series.

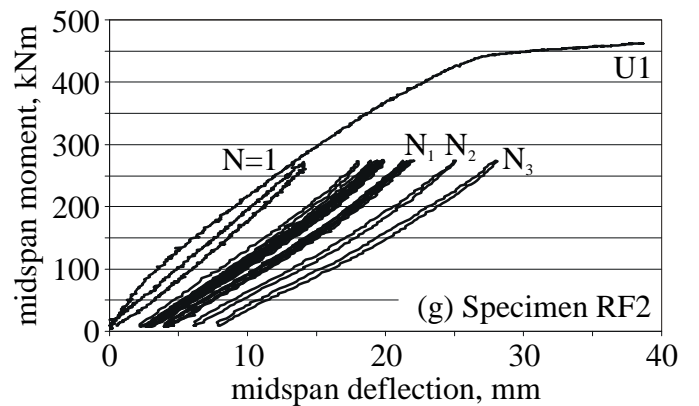
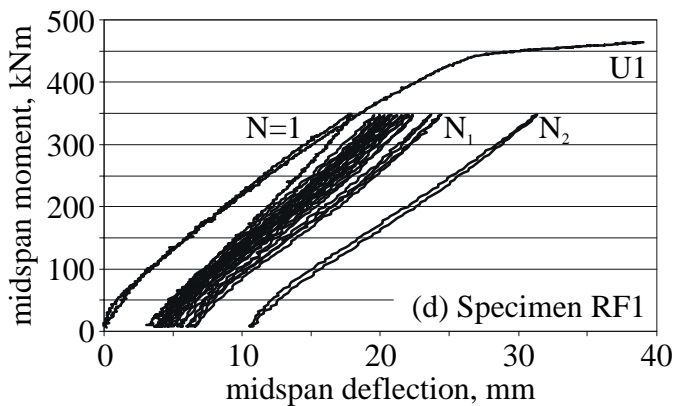
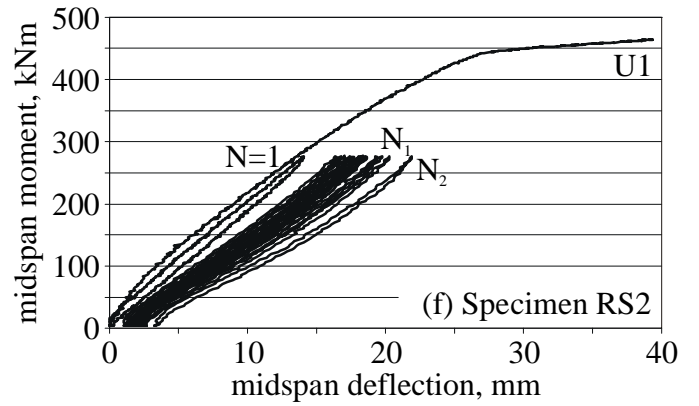
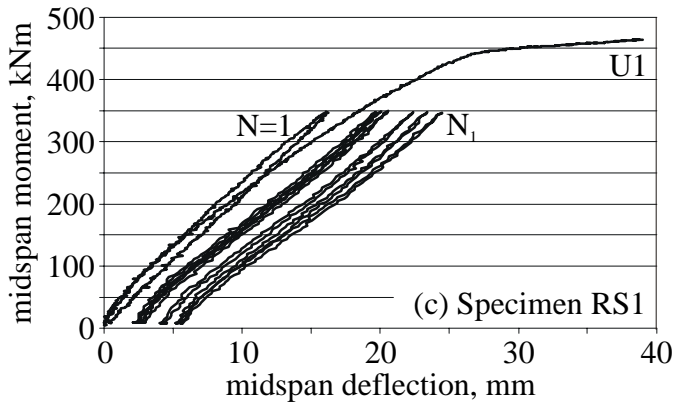
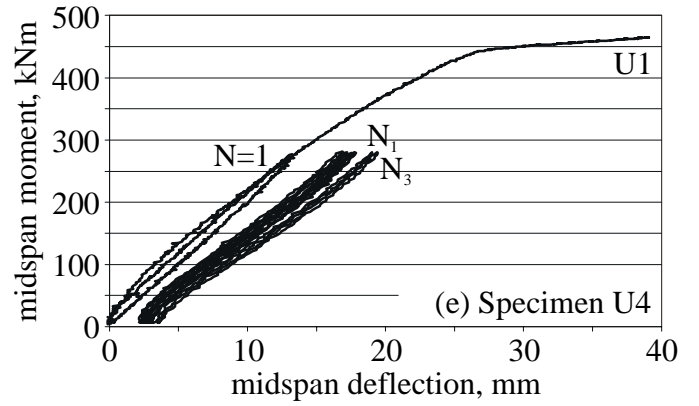
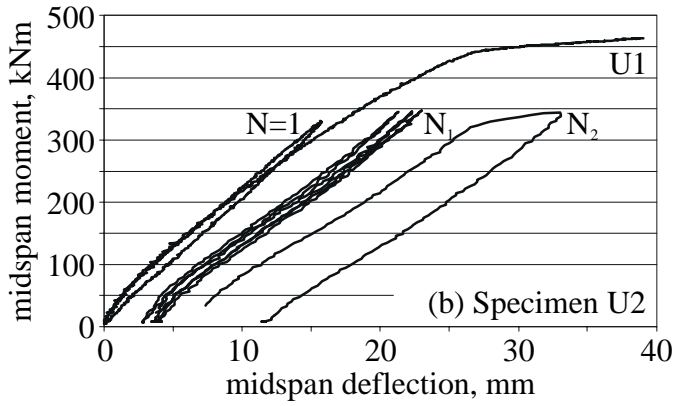
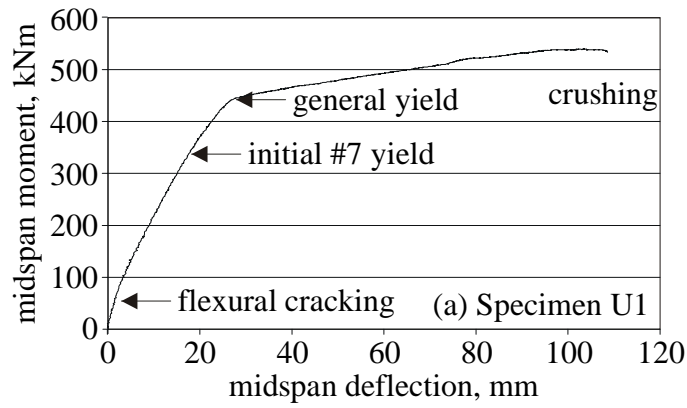


**Figure 3.** Applied moment versus midspan deflection responses of beams

### ***Endurance Limit (Specimen U3)***

Not reported in Table 1 or Figure 3, Specimen U3 was an unretrofit specimen tested at a low stress level to establish the endurance limit for these beams. Specimen U3 was tested at an applied moment ranging from 19 to 200 kNm, approximately 46% of the yield capacity of Specimen U1. This loading corresponded to an average stress range on the #7 bars of 215 MPa. The fatigue life of this specimen exceeded  $2 \times 10^6$  cycles at this load level, establishing a data point below the endurance limit. The stress level in this test was then increased to that used in the low stress series (above). Specimen U3, survived an additional  $6 \times 10^5$  cycles at this increased stress level.

### ***Delamination of CFRP Materials***

Delamination of the CFRP materials from the concrete substrate was observed in all retrofit specimens. Delamination began near midspan and progressed, with cycling, toward the nearest support. Delamination was only observed on one side of midspan for each beam. “Delamination” generally occurred through the cement matrix rather than through the adhesive or CFRP itself. This indicates that, as with all similar applications, the bond, and thus capacity, is controlled by the tensile capacity of the concrete substrate.

Delamination was observed within the first  $10^5$  cycles for the high stress series and within the first  $2.5 \times 10^5$  cycles of the low stress series. Delamination of the “strip” retrofit was noted earlier than for the “fabric” retrofit in both cases. Assuming that the “fabric” and “strip” retrofits carry the same stresses, the bond required for the “strip” is twice that of the “fabric” since the “strip” is half the width of the “fabric”. Experimental observations would appear to support this, since, in both cases, the “strip” was noted to initiate delamination sooner than the “fabric”.

As the specimens were cycled, delamination progressed along the beam, driven partially by the crack distribution and shear deformations of the beam. This mechanism is described by Sebastian (2001) and shown schematically in Figure 4. As delamination progresses, the tensile stresses transferred to the FRP are again carried by the internal reinforcing steel. Thus, once delamination has progressed away from the midspan region, the fatigue behavior reverts to essentially that of an unretrofit beam.

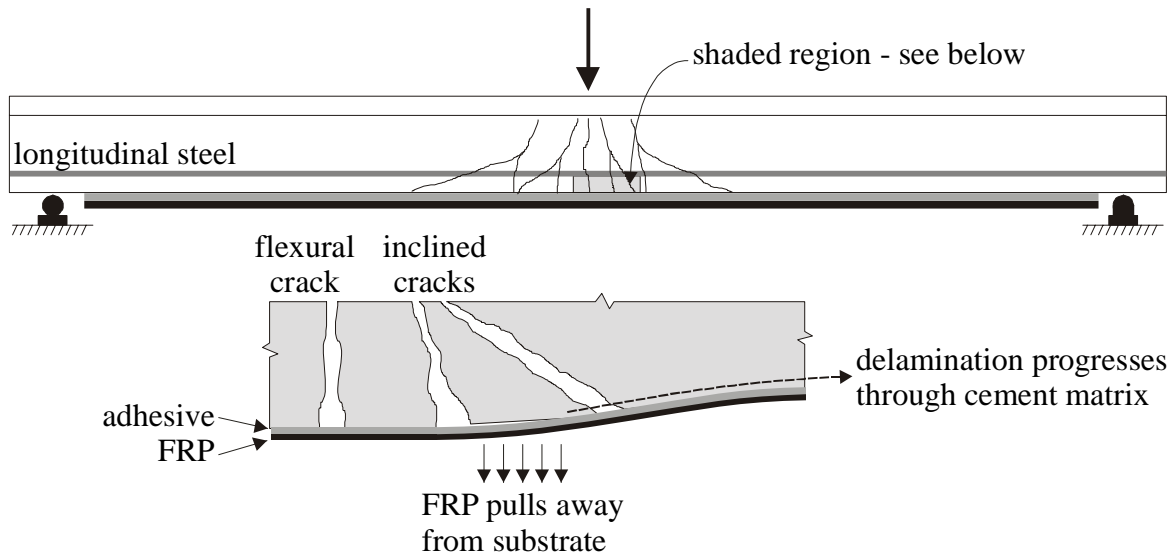


**Figure 4.** Delamination near midspan (after Sebastian, 2001)

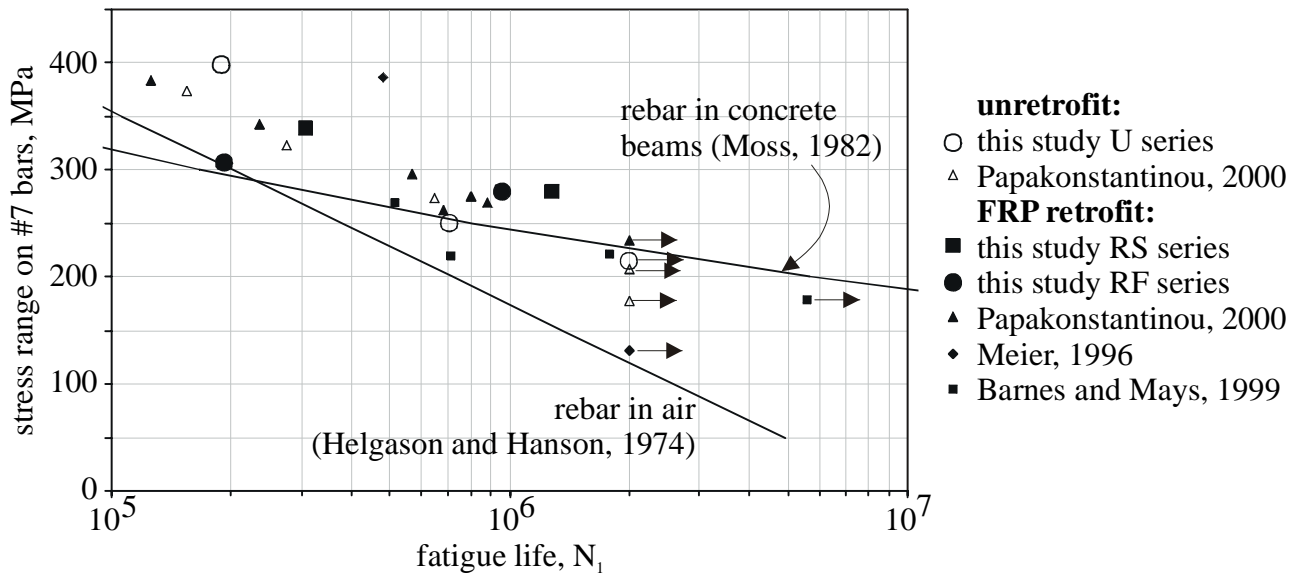


**Figure 5.** S-N results for reinforced concrete beams from this study and others

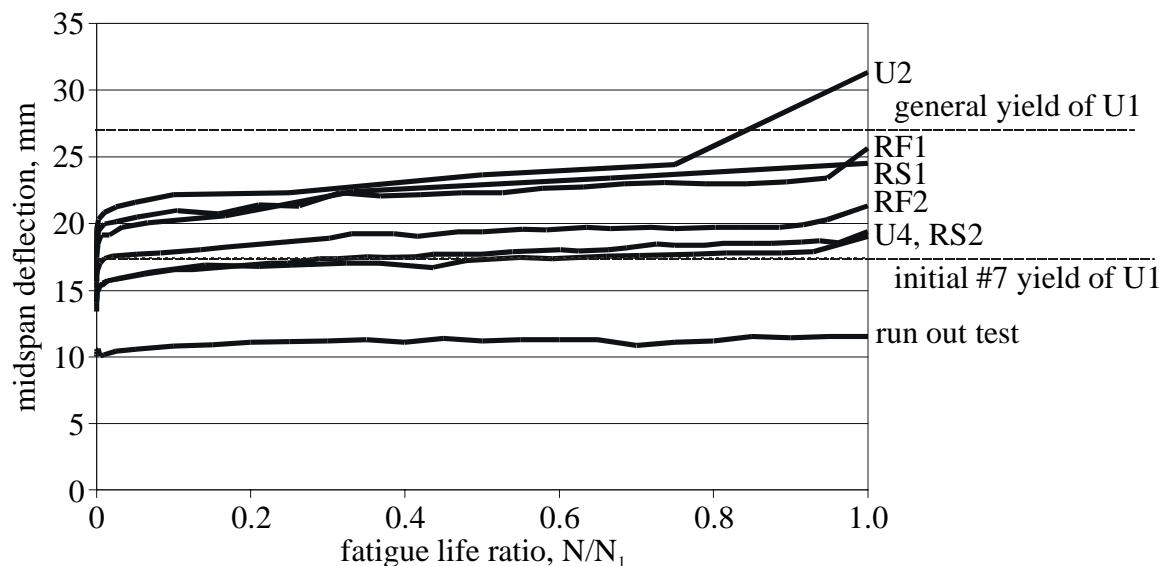
### S-N Behavior Of CFRP Retrofit Beams

Figure 5 plots the S-N results from this study (large symbols) and from comparable research involving FRP retrofit beams. The stress range plotted in Figure 5 is the stress in the extreme tension reinforcement in the original beam member. Also plotted on Figure 5 are established fatigue relationships for reinforcing steel in air (Helgason and Hanson, 1974) and in concrete beams (Moss, 1982).

The present specimens demonstrate behavior similar to that observed previously. The established relationships for the fatigue behavior of reinforcing steel appear to provide reasonable lower-bound estimates of fatigue life. Fatigue life increases as the stress range decreases and the application of the CFRP retrofit does extend the fatigue life. This improvement, however, is limited by the delamination of the CFRP from the concrete substrate. Initial observations support the conclusion that the “strip” retrofit exhibits better response under fatigue conditions. This may result from the improved quality control inherent in using a preformed strip.

Figure 6 shows the damage accumulation response, illustrated using the midspan deflection of the beam, plotted against the fatigue life ratio ( $N/N_1$ ). The curves shown display typical behavior: an initial accumulation of damage in the first 5% of the fatigue life, followed by a slow continued accumulation throughout the life. A final, rapid accumulation of damage in the last 5% of the fatigue life provides some warning of insipient failure.

As can be seen in Figure 6, the actual midspan deflection at failure is less than that corresponding to yield of the monotonically loaded beam (U1). Furthermore, the ultimate deflection is proportional to the applied stress level. The rate of accumulation of damage during most of the fatigue life – the slope of the curve between about  $0.1N_1$  and  $0.8N_1$  – is also proportional to the applied stress range, indicating that the progression of CFRP delamination is proportional to the applied load level.



**Figure 6.** Fatigue life ratio versus midspan deflection relationships

## Conclusions

The fatigue behavior of large-scale reinforced concrete tee beams retrofit with unidirectional CFRP materials on their stem soffits was investigated. It has been shown that the fatigue behavior of such retrofit beams is controlled by the fatigue behavior of the reinforcing steel. The fatigue life of a reinforced concrete beam can be increased by the application of an FRP retrofit, which relieves some of the stress carried by the steel. Thus, it is important that the FRP retrofit be as stiff as possible. For this reason, carbon FRP, rather than glass is preferred.

The observed increase in fatigue life, however, is limited by the quality of bond between the CFRP and concrete substrate. Delamination, initiating at midspan and progressing to a support is common and is driven partially by the crack distribution and shear deformations of the beam. Once delamination has progressed, stresses are no longer transferred to the CFRP and the fatigue behavior of the beam reverts to that of an unretrofit beam.

Improved bond characteristics including unique FRP reinforcing arrangements and the provision of mechanical anchorage into the confined concrete core will be investigated in the future. Additionally, the effect of controlling shear deformations of the beam by applying additional shear retrofit measures will be investigated. It is anticipated that controlling shear deformation will also serve to control the delamination of the flexural retrofit measures.

## Acknowledgements

This research is supported by the South Carolina Department of Transportation and the National Science Foundation (CMS 9908293). The support of Ed Fyfe and Sarah Cruikshank of Fyfe Co., San Diego CA is gratefully acknowledged.

## References

1. Barnes, R.A. and Mays, G.C. (1999). "Fatigue Performance of Concrete Beams Strengthened with CFRP Plates". *ASCE Journal of Composites in Construction*, Vol. 3 No. 2, pp 63-72.
2. Bentz, E. (2000). "REPSONSE 2000" version 1.0.0. University of Toronto.
3. Helgason, T. and Hanson, J.M. (1974). "Investigation of Design Factors Affecting Fatigue Strength of Reinforcing Bars – Statistical Analysis". *Abeles Symposium on Fatigue of Concrete*, American Concrete Institute SP 41, pp 107-138.
4. Mallet, G. (1991). *Fatigue of Reinforced Concrete*. Transport and Road Research Laboratory (TRRL) State of the Art Review / 2. United Kingdom. 166 pp.
5. Meier, U., Deuring, M., Meier, H. and Schwegler, G. (1992). "Strengthening of Structures with CFRP Laminates: Research and Applications in Switzerland". *Proceedings of Advanced Composite Materials for Bridges and Structures I*. Canadian Society of Civil Engineering.
6. Moss, D.S. (1982). "Bending Fatigue of High-Yield Reinforcing Bars in Concrete". *TRRL Supplementary Report No. 748*. Transport and Road Research Laboratory, Crowthome, UK.
7. Papakonstantinou, C.G., Petrou, M.F., and Harries, K.A., (2001). "Fatigue of Reinforced Concrete Beams Strengthened with GFRP Sheets", *ASCE Journal of Composites in Construction*, Vol. 5 No. 4, pp 246-253.
8. Sebastian, W.M. (2001). "Significance of Midspan Debonding Failure in FRP-Plated Concrete Beams". *ASCE Journal of Structural Engineering*, Vol 127, No. 7. pp 792–798.
9. Shahawy, M. and Beitelman, T.E. (1999). "Static and Fatigue Performance of RC Beams Strengthened with CFRP Laminates". *ASCE Journal of Structural Engineering*, Vol 125, No. 6. pp 613-621.

**Table 1.** Material properties, test parameters and predicted and observed fatigue behavior

	<b>Specimens</b>						
	<b>control</b>	<b>high stress series</b>			<b>low stress series</b>		
	<b>U1</b>	<b>U2</b>	<b>RS1</b>	<b>RF1</b>	<b>U4</b>	<b>RS2</b>	<b>RF2</b>
<b>retrofit</b>	none	none	strip	fabric	none	strip	fabric
<b>loading</b>	mono	1 Hz	1 Hz	1 Hz	1 Hz	1 Hz	1 Hz
<b>Material Properties</b>							
<b>concrete <math>f_c'</math>, MPa</b>	27.4	27.4	24.8	26.6	34.2	24.8	26.6
<b>#7 steel properties</b>	$f_y = 439$ MPa; $f_u = 740$ MPa						
<b>FRP <math>f_r</math>, kN/mm-ply</b>	na	na	5.3	0.875	na	5.3	0.875
<b>FRP <math>E_r</math>, kN/mm-ply</b>	na	na	294.4	72.5	na	294.4	72.5
<b>Retrofit Properties</b>							
<b>strength, kN</b>	na	na	540	355	na	540	355
<b>stiffness EA, kN</b>	na	na	30024	29646	na	30024	29646
<b>Test Control Parameters</b>							
<b>min. applied moment, kNm</b>	440 (yield)	63	63	63	25	43	12
<b>max. applied moment, kNm</b>	538 (ult.)	351	351	351	282	276	276
<b>Predicted Response Values</b>							
<b>yield capacity, kNm</b>	401	401	444	435	402	444	435
<b>ultimate capacity, kNm</b>	439	439	532	472	452	532	472
<b>min. #7 strain, <math>\mu\epsilon</math></b>	na	168	125	133	49	8	25
<b>max. #7 strain, <math>\mu\epsilon</math></b>	na	2179	2016	2098	1691	1535	1608
<b>#7 stress range, MPa</b>	na	402	378	393	328	305	316
<b>deflection at max. moment, mm</b>	27.9 (yield)	20.1	19.6	19.8	15.0	14.7	15.2
<b><math>N_1</math> (EQ 1)</b>	na	54000	74000	61000	140000	187000	163000
<b>Observed Response Values</b>							
<b>min. #7 strain, <math>\mu\epsilon</math></b>	na	290	210	160	17	0	0
<b>max. #7 strain, <math>\mu\epsilon</math></b>	na	2280	1900	1900	1263	1393	1393
<b>#7 stress range, MPa</b>	na	398	338	306	249	279	279
<b>deflection at max. moment; <math>N = 1</math>, mm</b>	26.9 (yield)	15.6	16.0	17.8	13.2	14.0	14.0
<b><math>N_1</math></b>	na	190000	308879	193160	710000	1280000	960000
<b><math>N_2</math></b>	na	194172	-	221083	800415	1580000	1280000
<b><math>N_3</math></b>	na	-	-	-	800415	1601773	1360000
<b><math>N_4</math></b>	na	-	-	-	-	-	1383018